JOURNAL OF MATERIALS SCIENCE 23 (1988) 3910–3920

Morphological and mechanical properties of extruded polypropylene/nylon-6 blends

PATRICK VAN GHELUWE, BASIL D. FAVIS, JEAN-PIERRE CHALIFOUX
National Research Council Canada, Industrial Materials Research Institute, 75 De Mortagne Blvd., Boucherville, Quebec, Canada, J4B 6Y4

Blends of polypropylene and nylon-6 extruded into ribbons at varying draw ratios generated laminar morphologies under our conditions. For the binary system, the size and distribution of the dispersed phase is coarse. The addition of an ionomer to the nylon prior to blending compatibilized the phases and produced much finer domains. The tensile properties of the virgin matrix material respond to the draw ratio in a parabolic manner attaining a maximum at intermediate values. Blending with nylon-6 attenuates the effect without improving the tensiles markedly. The compatibilized system however demonstrates greatly improved mechanical properties.

1. Introduction

Most polymer blend processing will afford a two-phased system where the equilibrium morphology is composed of spheres of the minor component dispersed in the major component, the matrix. Such systems yield better to quantitative analysis in terms of morphology or mechanical properties and consequently have been examined to some extent [1–10].

Blend morphology is dependent on a number of factors. Firstly, composition, viscosity ratio and elasticity may determine which of the components is the dispersed phase and ultimately where phase inversion will occur [2, 8]. The materials themselves, by their temperature dependent relative viscosities [3, 5, 8, 9], by their *relative* interfacial tension [7] and their elastic properties in the melt [5, 6, 8, 9] will determine the ease of obtaining a more or less fine dispersion. Finally, the compounding method and the processing conditions will influence the morphological outcome [5].

The morphology of these blends will in turn determine the mechanical properties of the blend [2, 5]. For instance, PE (polyethylene) in PC (polycarbonate) blends after compression moulding can be visualized as loosely fitting spheres in the PC matrix [4]. Due to poor interfacial adhesion, mechanically this blend behaves as a PC matrix containing empty holes and Young's modulus then decreases with an increase in PE. On the other hand PS–PC blends are composed of compactly embedded PS (polystyrene) spheres in the PC matrix. Consequently, PS contributes substantially to the modulus of the blend. Tensile strength and impact strength for these blends have been modelled on power laws of volume fraction of the dispersed phase.

Relatively little work has been reported on systems containing a dispersed phase having different morphologies such as fibre, platelet or ribbon structures. Fibrilar or rod-like features are occasionally observed [4] but have not been systematically analysed.

The uniaxial stretching of films extruded from molten blends of PS in PE show oriented domains [10]. As the amount of draw is increased during the processing the fibres become thinner and longer.

Extrusion of blends through capillaries may produce strands containing fibres of the dispersed component of the incompatible blend [11–13]. The viscosity ratio of the dispersed to matrix phases needs to be close to unity under the specific processing conditions for the formation of fibres to be observed. For lower values of the viscosity ratio finer and longer fibres are obtained but if the ratio becomes much greater than unity, shorter fibres and undeformed structures are produced.

Fibre formation is also dependent on the shear stress applied during the process [12, 16, 17]. The inherent rheological properties of the component materials also influence the appearance of the structural features in the dispersed phase. For instance, higher die swell correlated with an increased number of thinner fibres [12]. This observation also corresponds to the condition where the viscosity ratio is close to unity.

Platelet and layered structures can also be obtained by film extrusion or blow molding from dry blends of modified nylon and PE [14, 15]. No processing details are given but the particular morphology is certainly dependent on a low mixing–shearing history during the melting step prior to extrusion. Nylon is an excellent barrier resin and small amounts well distributed in a layered structure throughout a polyolefin will then greatly improve resistance to hydrocarbon vapour.

The understanding of the factors controlling more complex morphologies is still very limited. The interest lies in the varied possibilities for the design of composites having improved physical and mechanical properties over the constituent polymers. Especially when the dispersed phase adopts ribbon and platelet

0022–2461/88 $03.00 + .12

TABLE I Materials used (data obtained from the suppliers)

Material	Identifier	MI (g per 10 min)	Density ($g cm^{-3}$ at 250° C)	Tensile strength (MPa)
Pro-Fax 6701*	PP	0.8	0.750	35.2
Zytel 211†	Z	–	0.962	40.7
Surlyn 9020†	S	1.0	0.740	26.2

*T.M. Himont
†T.M. Du Pont

structures, its shape and dimensional characteristics will have an important bearing on the transport properties of small molecules through the blend [18].

Both polypropylene and nylon-6 are widely used film forming polymers [19]. Blending to produce a composite having a polypropylene matrix and a nylon dispersed phase provides an opportunity to ally the interesting mechanical properties of the former with the outstanding barrier properties of the latter. Most blending of polypropylene is with elastomers to achieve toughness [20].

Recent reports pertaining to blends of nylon-6 with polyolefins remain rather scarce [18, 21–29]. The studies either aim at getting a grasp of the morphologies controlling the barrier properties [18] or impact and mechanical strength properties [21, 22, 26, 27, 29]. Others address the rheological aspects of the blend and the process that will allow control of the morphology [23, 25, 28].

Here we report on the tensile properties of ribbons produced by melt extrusion of blends of polypropylene and nylon-6 at two concentrations (90/10 and 70/30) by weight. Similar blends with an ionomer modified nylon-6 are also examined. Stretching and calendering of the molten extrudate produced ribbons with a high uniaxial orientation with a minor transverse orientation component. The whole process generates highly laminar morphologies.

2. Experimental Procedure

2.1. Materials

Polypropylene was a standard extrusion grade, Pro-Fax 6701™ obtained from Himont in powder form.

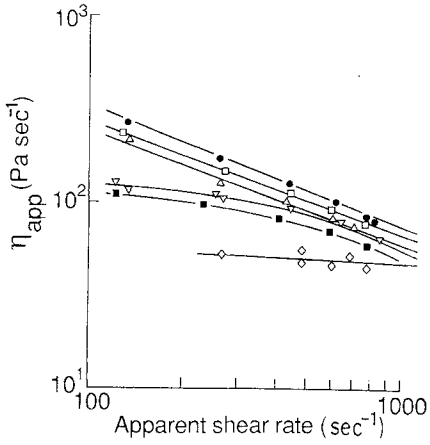

Figure 2 Apparent viscosity as a function of apparent shear rate at the wall at 250° C (● PP, □ PP PA10, △ PP PA30, ▽ ZS, ■ PP Z10, ◇Z).

To facilitate blending with other materials in granular form it was pelletized after extrusion using a Werner Pfleiderer ZSK30 twin screw extruder. Antioxidants were also incorporated at this stage (Ciba Geigy Irganox™ 1010 and 1024, 0.1% respectively).

Nylon-6 was Zytel 211™ obtained from DuPont in granular form. In every case the granules were dried in a vacuum oven at 80° C overnight.

Surlyn 9020™ obtained from DuPont was used as a compatibilizer at a level of 5% by weight in the nylon-6. The pelletized terpolymer (poly(ethylene-co-methylacrylate-co-butylacrylate)) is an ionomer with a zinc counterion. Prior to blending the material was also dried as described.

Some relevant material properties are shown in Table I.

2.2. Blending

Blends containing 10 and 30% by weight of nylon in polypropylene (hereafter noted PP Z10 and PP Z30) were prepared on the WP ZSK30 extruder. The granular mix of the two polymers was fed using an Acrison feeding hopper at a rate suitable to stay within the torque limit at 300 r.p.m. An ascending temperature profile was maintained in the barrel up to the die which was held at 250° C. To minimize

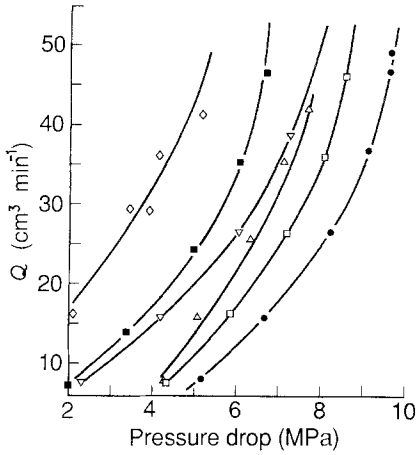

Figure 1 Volumetric flow rate as a function of pressure drop in the die at 250° C (● PP, ■ PP Z10, □ PP PA10, △ PP PA30, ◇ Z, ▽ ZS).

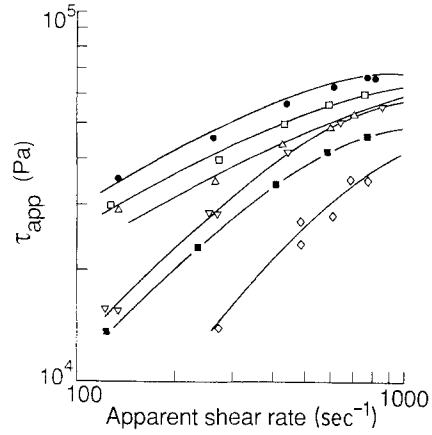

Figure 3 Apparent shear stress τ_{app} as a function of apparent shear rate at 250° C. (● PP, ■ PP Z10, □ PP PA10, △ PP PA30, ◇ Z, ▽ ZS).

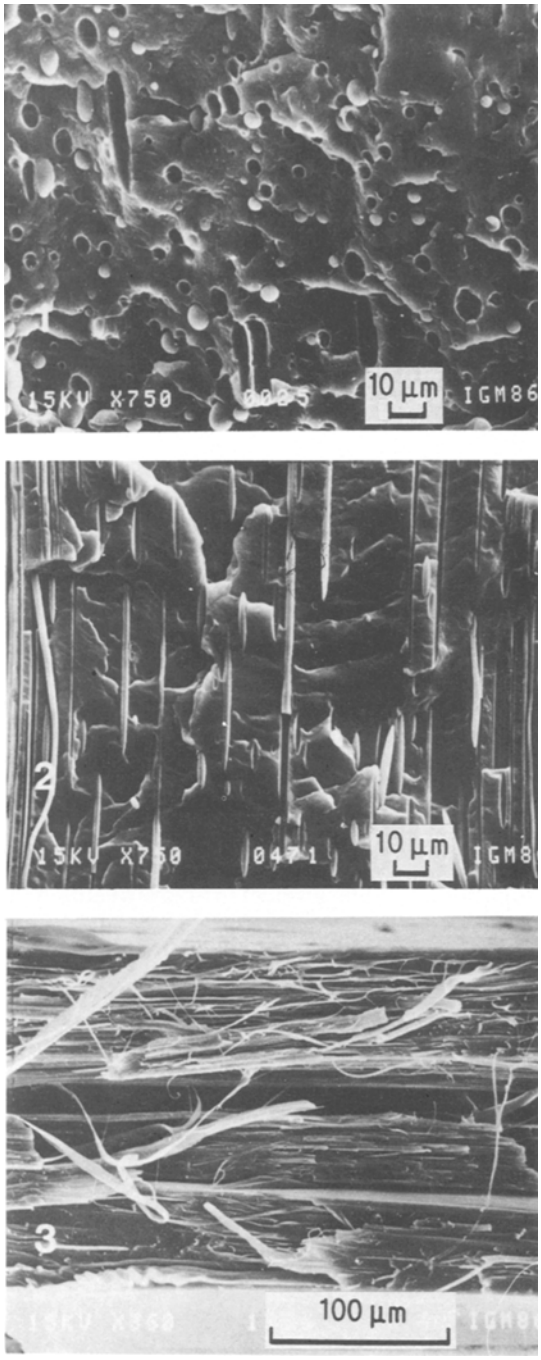

Figure 4 Schematic of the process layout. SEM photographs show morphology of ribbon at the position indicated. The blend illustrated is PP Z10.

degradation, a nitrogen atmosphere was imposed in the feed zone while the fourth and last zone was evacuated. The extrudates were quenched in cold water and immediately granulated.

Blends containing 10 and 30% modified nylon (hereafter noted PP PA10 and PP PA30) were obtained in a similar manner. The nylon was modified in a prior operation with the ionomer resin.

2.3. Ribbon extrusion

Ribbons of the five materials thus prepared were extruded through a 7.6 cm slit die with an adjustable gap at 250° C using a Brabender single screw extruder. The gap (H) was set at 0.011 in. (0.0279 cm) and the lip had a length (L) of 0.810 in. (2.0447 cm) for an L/H of 73. The screw had a 0.75 in. diameter (D) and a 3 : 1 compression ratio with an L/D of 25. Screw speed was 60 r.p.m. in all cases. The extrudate was taken up between water cooled steel rolls (5 inches diameter) having a polished chrome surface. The take up device also had two pinching pull rolls. Stretching was varied by adjusting the speed of the take up device. In each case the linear velocity of the extrudate (V_E) was calculated taking into account the melt density. The linear velocity of the rolls (V_R) was also calculated for each run. The hot stretch ratio (HSR) is then defined as $\text{HSR} = V_R - V_E/V_E$.

2.4. Tensile testing

Samples for mechanical testing in the machine direction only were obtained by punching using an ASTM D1708 die. Blends containing 30% nylon were difficult to sample, especially the low HSR ribbons which tended to delaminate when cut. To overcome this, more samples were cut and the better ones were chosen. The tensile curves for this blend were consequently less reproducible. Under these conditions the relative error on the tensile data is in the order of 20%. For virgin material and the compatibilized blends the error is 5%. The conditioned dogbones were drawn at room temperature on an Instron apparatus at a cross head speed of 2 mm min^{-1}. At this strain rate samples of the virgin polymer and its blends with the compatibilized systems tended to have very high elongations. Ultimate tensile properties were thus not obtained. In turn, this traction speed allowed a more ductile behaviour to be observed for those samples having high uncompatibilized nylon loadings. Otherwise they failed in a brittle mode and were quite sensitive to imperfections.

The stress–strain data were accumulated using the Instron software. The program gives secant modulus, stress at yield by the slope threshold method, strain at yield as well as area under the curve up to the yield point. The slope threshold corresponds to the point where the ratio of the slope of the stress–strain curve over the slope of the linear portion reaches a value of 0.3, as we chose.

2.5. Scanning electron microscopy (SEM)

Small strips cut from the ribbons were fractured at liquid nitrogen temperature. These samples were then vacuum metallized and examined with a JEOL 35 CF instrument. Thick samples fractured easily but thin samples would not and were thus notched prior to fracture.

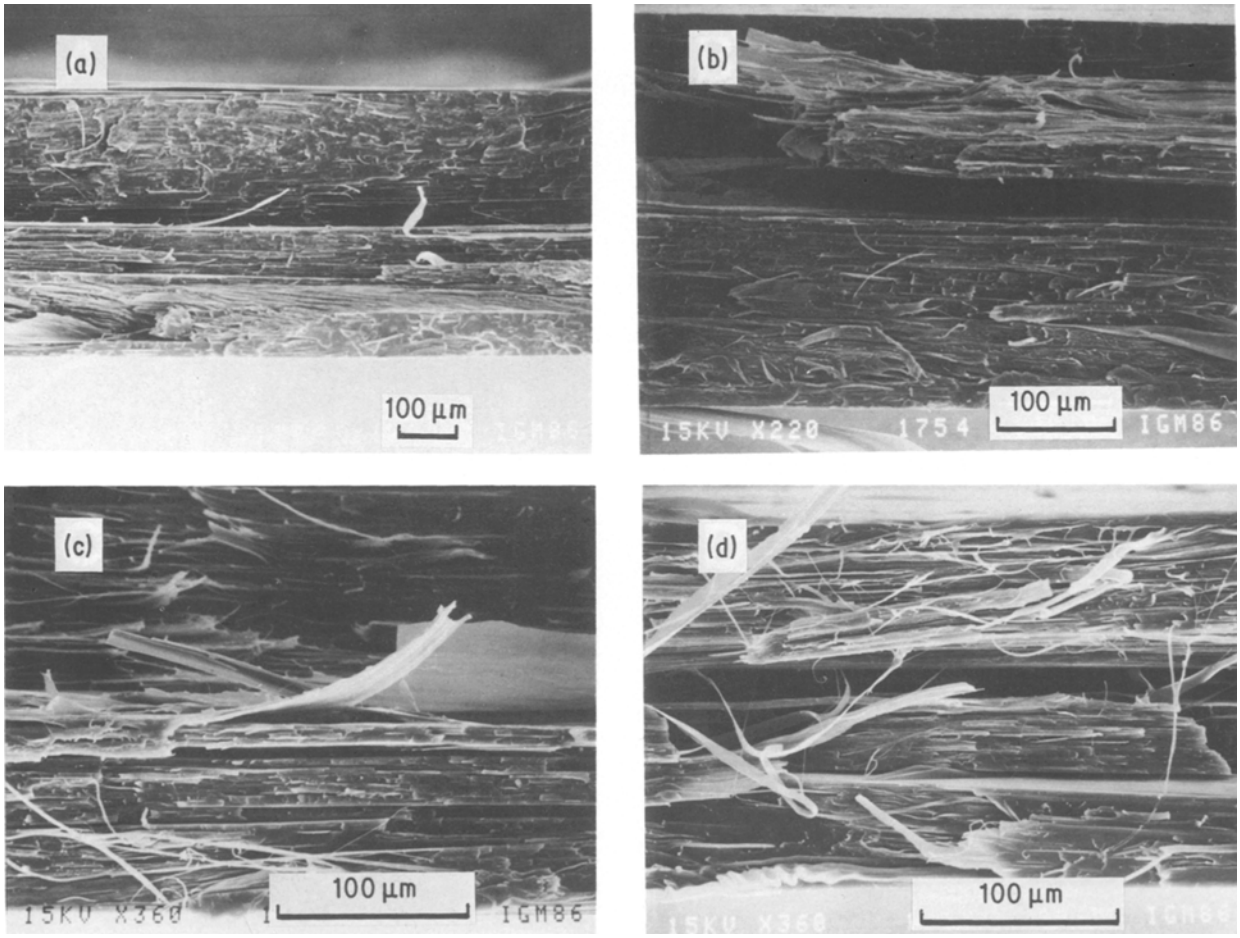

Figure 5 SEM of the PP Z10 blend at a HSR of (a) 0.5; (b) 2.0; (c) 4.1; (d) 5.6. Fracture surfaces are parallel to the machine direction and show the complete cross-section.

3. Results

3.1. Flow behaviour

Using the relationship between volumetric output and pressure drop in the slit die the apparent rheological parameters of the materials were obtained [30].

The volumetric extrusion rate as a function of pressure drop is shown in Fig. 1. The blend materials in every case lie between the curves of the base materials PP and Z.

A similar ordering is also found for apparent viscosity and apparent shear stress as a function of apparent shear rate, Figs 2 and 3. The viscosity curves for PP, PP PA10 and PP PA30 adopt a linear relationship while those of PP Z10 and ZS (Zytel Z11™ and Surlyn 9090™ 95/5) approach Newtonian behaviour at low shear rates. Over the range of shear rates examined the pure nylon-6 (Z) had Newtonian flow properties with the lowest viscosity.

At the extrusion rates used (60 r.p.m.) to produce the ribbons, the viscosity ratios of the dispersed phase to that of the matrix were 0.46 for nylon-6 in PP and 0.76 for modified nylon-6 in PP. The addition of 5% by weight of the ionomer compatibilizer to the nylon increased the viscosity of this modified nylon considerably. Within the range of shear rates examined, the apparent viscosity of the modified nylon remained higher than that of the PP Z10 blend itself.

3.2. Morphology

As the blends are extruded and drawn through the calender rolls, the morphology of the dispersed phase undergoes drastic transformations as shown in Fig. 4. At the exit of the die the shape of the dispersed nylon phase is largely spherical. Only at high extrusion rates do elongated morphologies begin to appear at the die exit.

In the drawing zone between the die and the calender rolls, the molten ribbon experiences elongational forces leading to the formation of a neck. In this region the droplets are deformed to fibrillar structures in the molten matrix.

When the elongated extrudate enters the calender with the maximum closing pressure applied to the rolls, the thickness of the ribbon is further reduced. This also induces a transverse elongational component in the already drawn strip. At this stage the overall morphology of the ribbon adopts a highly layered structure throughout as shown in the third photo of the figure.

HSR's were varied between 0 (for equivalent extrudate and take-up velocities) and about 10 which corresponds to the ultimate drawing velocity where handling a thin static-charged ribbon becomes difficult. This draw ratio is not the maximum attainable with these materials although it also represents the approximate condition where the width of the ribbons begin to vary periodically (draw resonance) [31].

As the HSR of PP Z10 and PP Z30 blends is increased the morphology of the ribbons evolves from a composite with a more or less homogeneous skin and

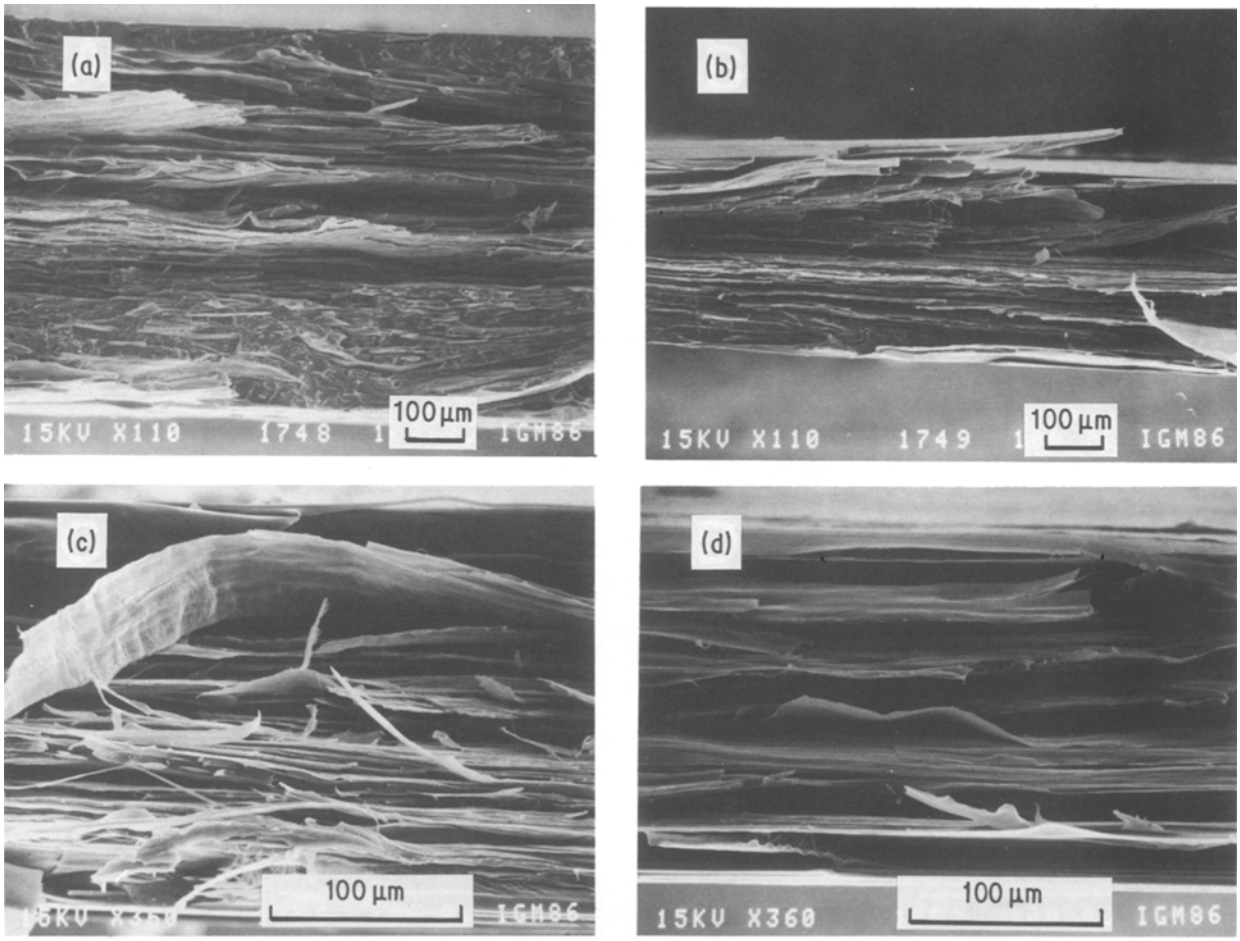

Figure 6 SEM of the PP Z30 blend at a HSR of (a) 0; (b) 1.9; (c) 4.6; (d) 7.0. Fracture surfaces are parallel to the machine direction and show the complete cross-section.

a layered core, to a completely layered structure (Figs 5 and 6). The highly aligned domains render the thicker ribbons susceptible to delamination while all are easy to tear along the axial direction.

SEM's of the fracture surfaces of virgin PP ribbons having a low and high HSR are shown in Fig. 7. At low HSR the appearance is that of a uniform brittle material while at high HSR the layered structure is slightly evidenced.

To examine the influence of the compatibilizer in comparison with the non-compatibilized system, the granular blends of both PP Z30 and PP PA30 were compression moulded. The fractured samples are compared in Figs 8a and b. It is seen that the spherical domains of the nylon blend have a wide size distribution (2–15 μm) with very clean fracture surfaces. On the other hand the fracture surface of the compatibilized nylon blend is seen to be of a much finer grain. The sphere size distribution is narrower with a much reduced domain size (2–4 μm).

Blends of PP/S and Z/S both in the proportion 70/30 were also compression moulded. Their fracture surfaces are shown in Figs 8c and d. It is evident that the PP/S blend at the indicated concentration is incompatible. The dispersed ionomer is seen as irregular domains of varying sizes with clean interfaces. On the other hand the blend with the nylon examined at the same magnification shows no discernible domains indicating compatibility at this scale.

Fracture surfaces obtained from ribbons of the compatibilized blends are shown in Fig. 9. For PP PA30 it can be seen that the layered structure is still present although at a much smaller size. The dispersed phase even at a level of 30% by weight is difficult to distinguish. For PP PA10, the layered structure is no longer apparent and the fracture surface very closely resembles that of virgin PP.

3.3. Mechanical properties

The modulus of the five materials (PP, PP Z10, PP Z30, PP PA10, PP PA30) as a function of HSR is shown in Fig. 10 for comparison. The matrix material PP is seen to go through a maximum at a HSR of approximately 2 and the non-compatibilized blends also go through a maximum but their modulus drops off at a much slower rate than HSR. Overall, the PP Z30 blend is inferior while the PP Z10 modulus remains higher than that of the virgin PP over the whole range of HSR.

The compatibilized blends PP PA10 and PP PA30 demonstrate a monotonic increase of modulus although at low draw ratios the value is inferior to that of PP. The increase in the modulus with HSR of the compatibilized blends is more or less parallel with the PP PA10 having the higher value throughout.

Stress at yield and the corresponding strain is compared in Figs 11 and 12 for all the materials. Here again the virgin matrix material is seen to undergo an

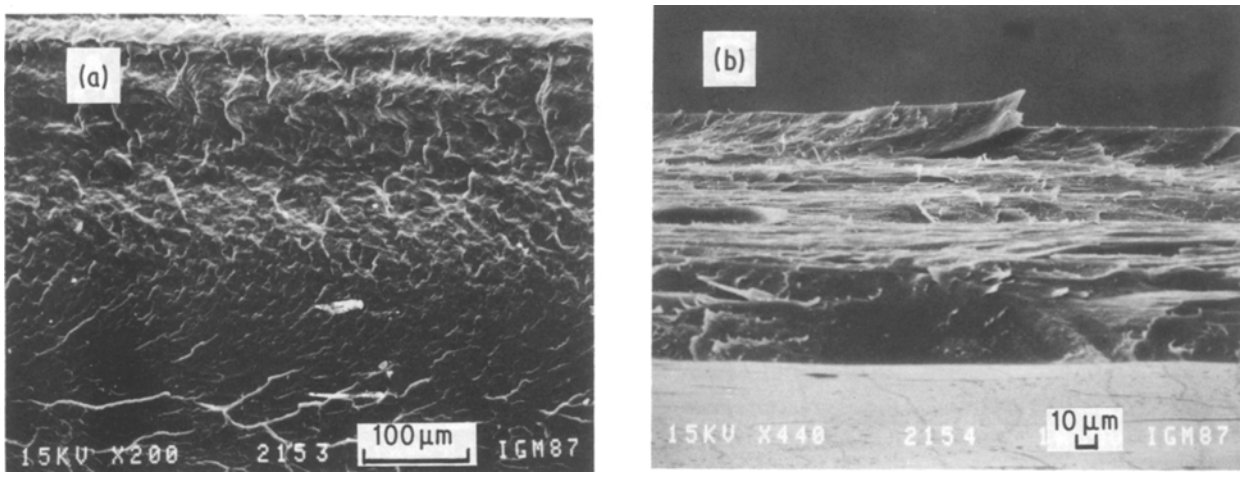

Figure 7 SEM of PP drawn at a low and high HSR (a) HSR 0.79 (b) HSR 5.26 (complete cross-sections are shown).

increase up to approximately a HSR of 2 followed by a decrease of these material properties. The non-compatibilized blends demonstrate the same trends although the maxima in the stress and strain values at yield are observed at a HSR of 4 to 5. For the compatibilized blends the stress and strain properties again increase monotonously with HSR. Stress at yield for the modified nylon blends parallels the PP values up to the onset of the property decrease for the matrix material. Stress at yield is higher for PP PA10 compared to the PP PA30 blend although the strain values are more or less similar. At high HSR the strain values seem to level off while for PP PA10 they show a tendency to also drop off at higher HSR values.

The area under the stress–strain curves up to the point of yield is also plotted against the HSR in Fig. 13. For the uncompatibilized system at the bottom, the values seem to coincide over the HSR range observed. At the upper end, the area values for the compatibilized system are also plotted. The two curves for the compatibilized system standout from the lower curve corresponding to the virgin matrix material which in this graph also closely approximates the behaviour of the non-compatibilized system.

4. Discussion

4.1. Morphology

4.1.1. Influence of the process

The micrographs of the PP/nylon-6 blends are typical of an incompatible system, (Figs 4–6). Within the RPM range examined in our process the shear rates spanned 10^2–10^3 (sec) and the uncompatibilized system still remained as a coarse dispersion at the exit of the die. At the highest shear rates little or no elongated structures were observed.

Fibrillation of the dispersed phase occurs in the neck of the drawn molten ribbon. Melt spinning of polymer blends also proceeds by the deformation of globules at the exit of the spinneret into fibrils in the spun fibre [32]. The amount of draw down during the spinning of PE–PS blends has been correlated with the diameter of the dispersed fibres [6]. It seems that the mean diameter of the fibrils does not reduce as quickly as would be expected from affine deformation. In other words the elongational flows of the matrix and dispersed phases are not directly coupled. Recently, it has been shown that the incorporation of a minor amount of an incompatible material to a molten polymer induces "orientation suppression" in the fibre spinning process [32]. The effect was shown to be related to the presence of droplets within the matrix. These can be compared to holes punched in an elastic sheet. Upon stretching, the holes deform and the material around them also. However, between the holes themselves much less deformation is observed. This should markedly influence the mechanical properties of our ribbons.

When the molten ribbon enters the calender rolls with a maximum of closing pressure applied, the fibres dispersed in the matrix are themselves then flattened to ribbons. The overall appearance of the composite then adopts a highly layered structure. The morphology of these extruded ribbons is akin to the laminar morphologies obtained with the DuPont process for barrier resins [14, 15]. Whereas the latter relies on low shearing–mixing to attain the lamellar structure, here the process is one relying on biaxial orientation. Since the aspect ratio of the dispersed phase is rather large, the axial elongation in the cross-machine direction is only minor. A more balanced bi-axiality could be obtained by blown film extrusion.

Drawing leads to a finer morphology. As the HSR increases, the extruded ribbon becomes thinner and the nylon in the dispersed phase is consequently more elongated (Figs 5 and 6). The aspect ratio of the dispersed nylon in the form of ribbons increases drastically. This is to be expected since the molten ribbon entering the calenders is thinner, there is then less material available to set up a suitable flow in the cross-machine direction between the rolls.

4.1.2. Influence of the composition

Composition of the incompatible blends usually has a morphological bearing [1, 3, 5–9]. This occurs through the influence of composition on the overall viscosity of the blend and on droplet coalescence–breakup interaction. Here, the higher concentration (PP Z30) leads to a coarser more layered structure as opposed to a

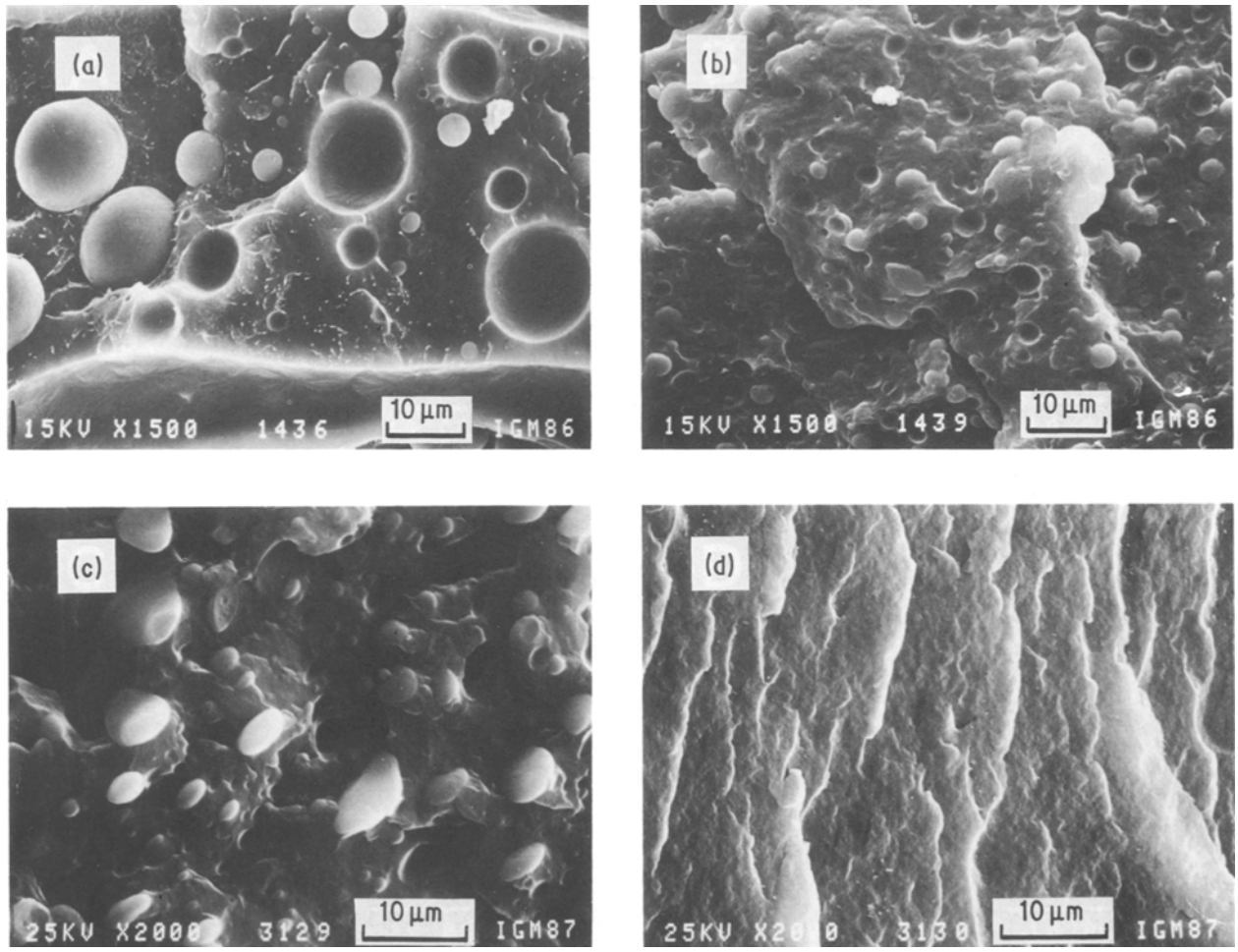

Figure 8 Brittle fracture surfaces of compression moulded samples using extrusion blended materials. (a) PP Z30; (b) PP PA30; moulded samples. Comparison of morphologies of (c) PP/S (70/30) and (d) Z/S (70/30).

finer more fibre-like structure for the lower concentration blend (PP Z10).

The nature of the dispersed phase, whether it is the pure nylon-6 or the compatibilized material, also influences the morphology. Two aspects seem to be of importance in this case: the degree of compatibility and the viscosity ratios of the phases. PP and Z are incompatible as visualized in the fractured compression moulded samples (Fig. 8a). Adding the compatibilizer changes the viscosity ratio while rendering the dispersed phase more shear sensitive. The Z/PP viscosity ratio goes from 0.46 to 0.76 for ZS/PP for apparent viscosities at 250° C and at 60 r.p.m. in our process. The viscosity ratio in the latter case affords a more uniform dispersion. It remains speculative whether the interface has also improved in this compatibilized blend. The ionomer blended at a level of 30% with the matrix phase (PP) and the dispersed phase (Z) does not seem to be compatible with the polyolefin but is much more so with the nylon-6 on the scale offered by the micrographs (Figs 8c and d).

4.2. Drawing and tensile properties

Here the complex morphology does not lend itself easily to analysis in terms of mechanical properties such as might be applied to spherical domains dispersed in a matrix [4]. The dimensions of the flattened and elongated structures in these extruded ribbons can only at present be evaluated in a qualitative way.

There is a definite influence of the rate of drawing on the tensile properties of the ribbons. For the matrix material drawing under the specified conditions is detrimental to the tensile properties beyond a HSR of 2. For the blended materials the effect is less and for the compatibilized blend, tensile properties improve with drawing. Very little data is available in the literature to correlate with the present observations. Stretching usually enhances polymer properties. The strength and ductility are improved by orientation in the hot or cold state [10, 33, 34]. It is generally agreed that melt spinning of high molecular weight polymers leads to filaments having dramatically increased mechanical properties [35, 36]. Also, films having unusual elasticities have been produced by inducing crystallization in the direction of the prevailing melt flow [37]. These crystalline platelet morphologies deform under stress by the formation of voids which are bridged by fibrils. Yet under some conditions drawing and orienting can produce a material with decreasing mechanical properties as the draw ratio is increased [38–40]. In fact, for each material and set of processing parameters there is an increase in the properties up to a certain draw ratio. Beyond this point a decrease is observed. For biaxially stretched acrylic sheet [38], the effect on the principal mechanical properties is discussed in terms of molecular orientation. Up to a certain draw ratio, the alignment of the molecules contributes toward a greater ordering throughout the

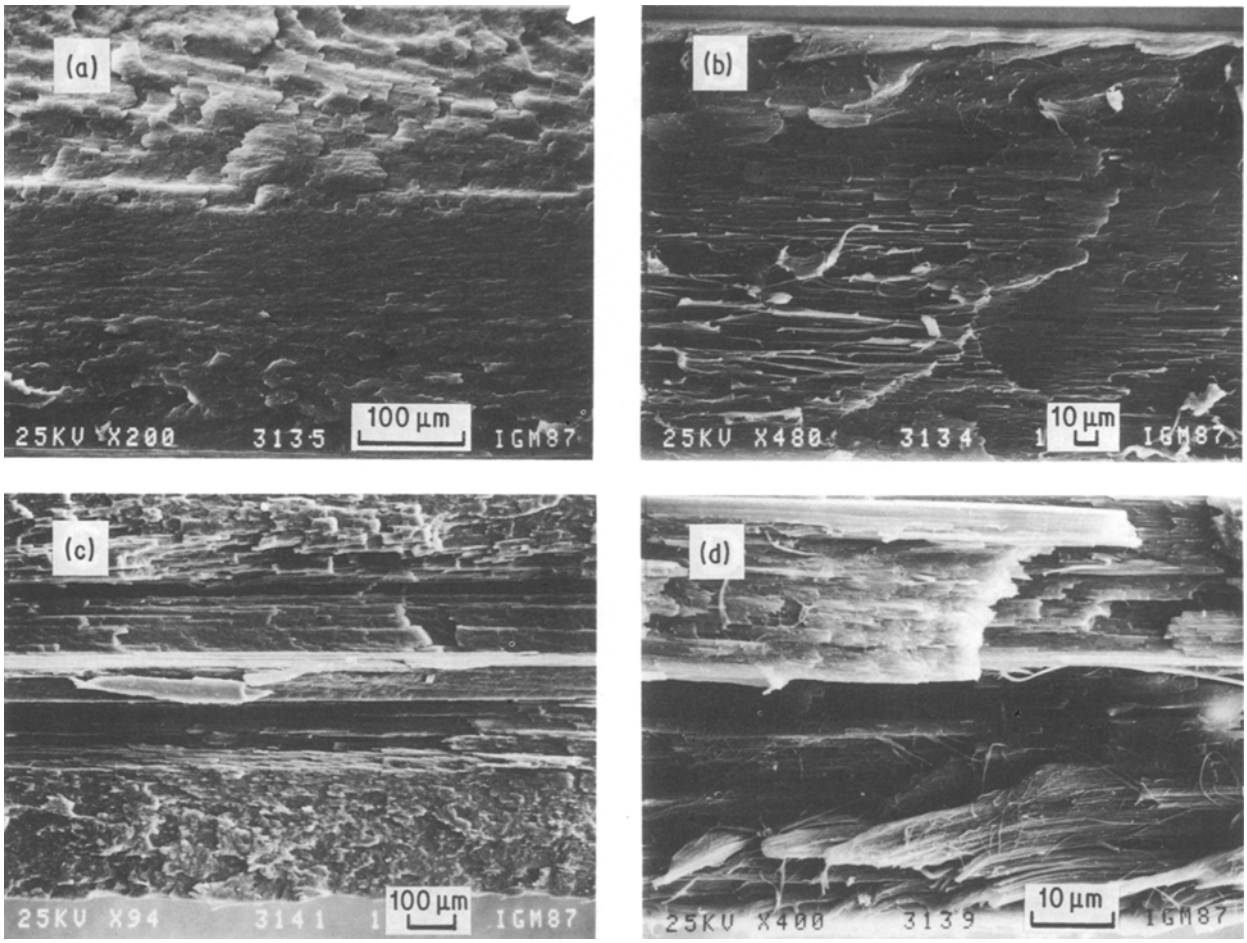

Figure 9 SEM of the PP PA10 blend at a HSR of (a) 0.60; (b) 6.43. SEM of the PP PA30 blend at a HSR of (c) 0; (d) 5.65.

structure. As stretching is increased a point is reached where flaws begin to appear between the oriented structures of the matrix. Thus U-shaped curves are obtained when plotting mechanical properties against drawing [39]. Wear resistance along different axes of an oriented polymer also responds in a similar way, initially increasing to a maximum and then decreasing again with draw ratio [40]. In the preparation of ultra high modulus polyethylene fibres by melt spinning, the onset of poor mechanical properties at precise draw ratios has been discussed in terms of void formation and fibrillation [36]. Higher temperatures as well as lower molecular weights increase the draw ratio attainable before the tensile properties begin to deteriorate.

This observation concerning the effect of molecular weight and temperature furthermore stresses the importance of achieving disentanglement if orientation is to be efficient. Untangled molecules are more efficient in the crystallization process. Once the lamellae have been constructed, minor orientation within the amorphous zones, still possible if the remnant chains are not too snarled, will achieve ultimate properties. The population of these tie molecules or tie fibrils

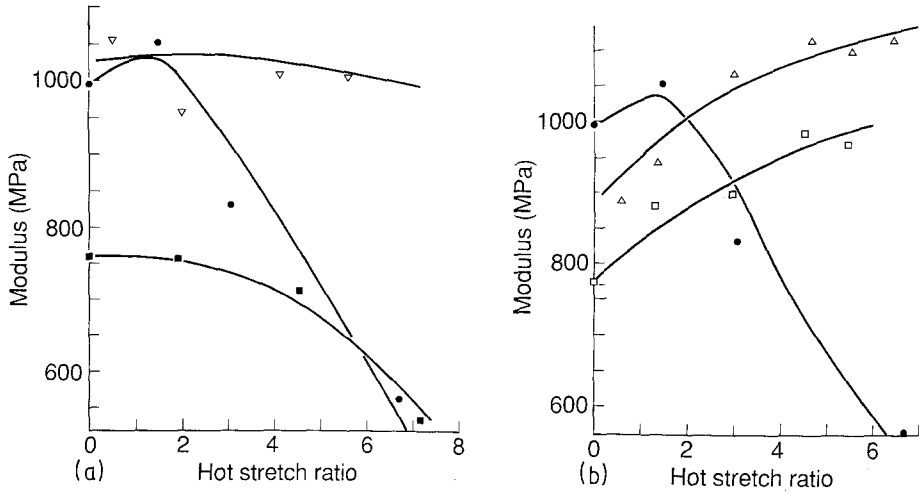

Figure 10 Modulus of the ribbons as a function of HSR (● PP, △ PP PA10, ■ PP Z30, ▽ PP Z10, □ PP PA30).

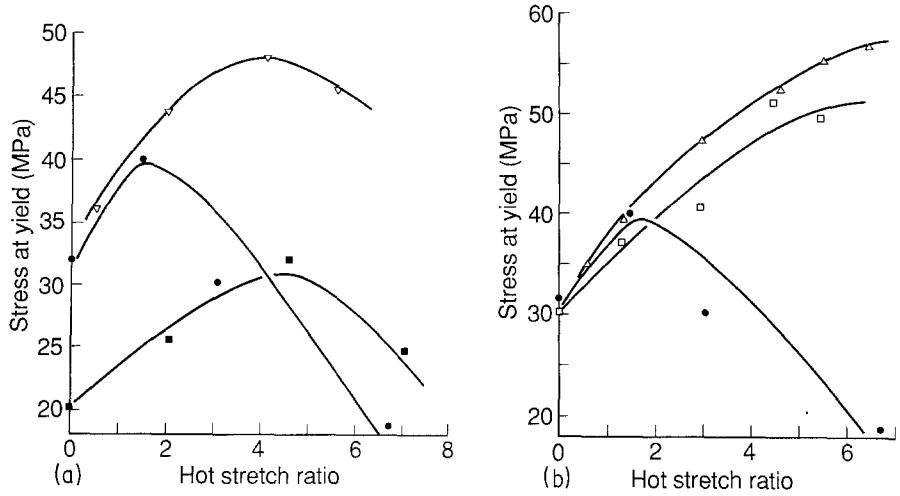

Figure 11 Stress at yield plotted against HSR (● PP, △ PP PA10, □ PP PA30, ▽ PP Z10 ■ PP Z30).

linking the crystalline zones of semicrystalline polymers has been related to the ductile to brittle transition observed for these materials [41].

In similar drawing experiments as described here [40], we have obtained tensile data on ribbons produced with a lower molecular weight isotactic PP (1.7×10^5 molecular weight as opposed to 3.6×10^5 for the present material and a polydispersity of 1.18 and 1.31 respectively). The yield stress and break stress values are plotted against HSR for both polypropylenes in Fig. 14. It is seen that for the lower molecular weight material extruded at the same temperature the tensile properties increase monotonically. Presumably extruding the higher molecular weight PP used in this study at still higher temperatures, or providing for a longer residence time at 250° C, would permit a more efficient alignment of the tie molecules in the virgin PP matrix. If this could be observed, it would stress the necessity of achieving proper disentanglement during or prior to elongation. The deliberate use of shearing to induce suitable disentanglement for modifying polymer melt properties has been discussed recently [43].

The outstanding feature in the tensile properties of these ribbons is the dramatic improvement in modulus and yield strength achieved with a relatively small amount of nylon-6. The extrusion-drawing of the PP ribbons produced a material having decreased properties. Under the same conditions but adding only 10% nylon-6, ribbons are obtained with acceptable tensiles over the HSR range. Then, if 10% of ionomer-modified nylon-6 is added, the properties considerably surpass those of the matrix material over the drawing range examined. HDPE and PS have been blended and extruded in a one-step process [9]. The tensile strength of the ribbons in most cases increased with HSR and the ductility expressed as the percentage elongation at break was found to go through a maximum with HSR. Because the molecular weights of their polyethylenes were lower they did not observe the U-shaped curves for the tensile properties of the virgin matrix materials. The tensile strength of their polystyrene levels off between a HSR of 2 and 4. This material, when blended with PE under specific conditions, then also leads to parabolic curves for the tensile properties as a function of HSR.

The presence of the ionomer in the nylon and its marked effect to improve the tensile properties should be discussed in terms of its effect on the overall crystallinity of the system and possibly also on the interface between the two incompatible components. Experimental evidence is not available at the moment to discuss these influences. However, in numerous instances, the presence of extraneous materials has been found to

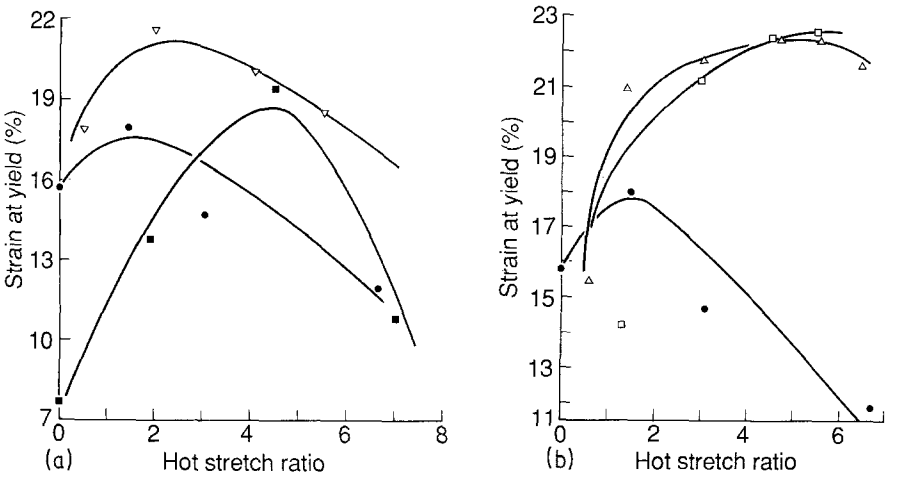

Figure 12 Strain at yield plotted against HSR (● PP, ▽ PP Z10, ■ PP Z30, △ PP PA10, □ PP PA30).

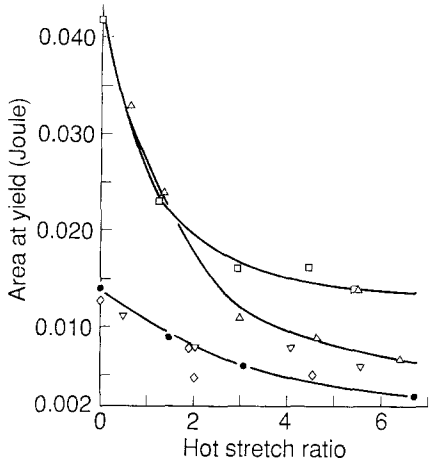

Figure 13 Area at yield plotted against HSR (● PP, ▽ PP Z10, ◇ PP Z30, △ PP PA10 □ PP PA30).

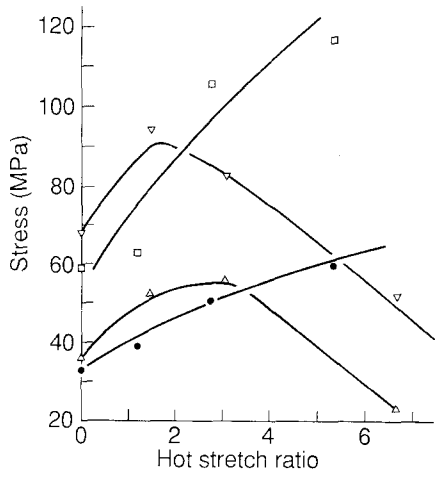

Figure 14 Yield and break stress plotted against HSR (● yield low molecular weight, □ break low molecular weight, △ yield high molecular weight, ▽ break high molecular weight).

affect the crystallization kinetics of polymer melts [44, 45]. Nylon or wood fibres when put in the presence of a PP melt induce preferential crystalline growth at their surfaces. These crystalline regions improve the mechanical properties of the fibre reinforced polymer systems. Also, flow induced crystallization of two-phased melts can obtain orientation in the fibrillar phase as demonstrated by its higher birefringence and melting point [44].

In terms of bulk properties, the result of adding the ionomer to the nylon phase increases the area under their stress–strain curves (Fig. 13). In the absence of microstructural information the actual mechanism can only be speculative. It is nonetheless made clear that these modified blends are mechanically very different from those of the binary blend by the behaviour of the curves in the figure. For the uncompatibilized system, the data points are grouped along a line in the low end of the energy scale. For the compatibilized system the points cover a larger energy band as a function of HSR. Up to a HSR of 2, both curves are similar. Beyond the draw ratio of 2, the area values level out to about 1.4×10^{-2} J for the 30% modified nylon blend and to 0.6×10^{-2} J for the 10% blend. The remarkable aspect is how both types of materials stand out from one another. The fact that all the data points for the binary blends are grouped at low energies along the same curve for the matrix material indicates poor stress transfer across the interface for this system as compared to the compatibilized system. Furthermore, morphologically, the dispersed phase in the former system is much coarser than in the three component system. Since ductility can usually be associated with a narrow distribution of fine particles and good interfacial adhesion this is well substantiated by our photographs of the fractured surfaces (Figs 8b and 9).

5. Conclusions

The extrusion-drawing of high molecular weight PP into ribbons can be detrimental to the mechanical properties in the machine direction. Under the same conditions adding 10% of an incompatible material (nylon-6) will give a product not affected by draw ratio. For higher concentrations (30%) of the dispersed phase the mechanical properties remain inferior and respond very little to draw ratio. The addition of 5% ionomer to the nylon dispersed phase leads to a much finer morphology and to extruded ribbons demonstrating increased mechanical properties with increasing draw ratios.

Acknowledgements

The authors wish to acknowledge the patience and technical ability of Ghislain Chouinard and Christian De Grandpré. The participation of Stéphane Bourgeois during the initial effort of this work is also gratefully recognized.

References

1. J. M. STARITA, *Trans. Soc. Rheol.* **16** (1972) 339.
2. W. M. BARENTSEN and D. HEIKENS, *Polymer* **14** (1973) 579.
3. D. HEIKENS and W. M. BARENTSEN, *ibid.* **18** (1977) 69.
4. T. KUNORI and P. H. GEIL, *J. Macromol. Sci.-Phys.* **B18** (1980) 93, 135.
5. A. P. PLOCHOCKI, *Polym. Engng Sci.* **23** (1983) 618.
6. K. MIN, J. L. WHITE, J. F. FELLERS, *J. Appl. Polym. Sci.* **29** (1984) 2117.
7. S. ENDO, K. MIN, J. L. WHITE and T. KYU, *Polym. Engng Sci.* **26** (1986) 45.
8. B. D. FAVIS, J. P. CHALIFOUX and P. VAN GHELUWE, *SPE Technical Papers* **33** (1987) 1326.
9. B. D. FAVIS and J. P. CHALIFOUX, *Polym. Engng Sci.* **27** (1987) 1591.
10. J. R. STELL, D. R. PAUL, J. W. BARLOW, *Polym. Engng Sci.* **16** (7) 496 (1976).
11. N. P. KRASMIKOVA, E. V. KOTOVA, G. V. VINOGRADOV and Z. PELZBAUER, *J. Appl. Polym. Sci.* **22** (1978) 2081.
12. M. V. TSEBRENKO, N. M. RENZANOVA and G. V. VINOGRADOV, *Polym. Engng Sci.* **20** (1980) 1023.
13. P. ALBIHN, P. FRANZEN, J. KUBAT and M. RIGDAHL, *J. Appl. Polym. Sci.* **32** (1986) 4837.
14. P. M. SUBRAMANIAN, *Polym. Engng Sci.* **25** (1985) 483.
15. P. M. SUBRAMANIAN and V. MEHRA, *ibid.* **27** (1987) 663.
16. V. E. DREVAL, G. V. VINOGRADOV, E. P. PLOTNIKOVA, M. P. ZABUGINA, N. P. KRASNIKOVA, E. V. KOTOVA and Z. PELZBAUER, *Rheol Acta* **22** (1983) 102.

17. J. J. ELMENDORP, *Polym. Engng Sci.* **26** (1986) 418.
18. M. R. KAMAL, I. A. JINNAH and L. A. UTRACKI, *ibid.* **24** (1984) 1337.
19. J. H. BRISTON, "Plastic Films", 2nd Edn, Longman, New York (1983) pp. 19, 51.
20. P. GALLI, S. DANESI and T. SIMONAZZI, *Polym. Engng Sci.* **24** (1984) 544.
21. F. IDE and A. HASEGAWA, *J. Appl. Polym. Sci.* **18** (1974) 963.
22. D. BRAUN and U. EISENLOHR, *Kunstoffe* **65** (1975) 9.
23. B. R. LIANG, J. L. WHITE, J. E. SPRUIELL and B. GOSWAMI, *J. Appl. Polym. Sci.* **28** (1983) 2011.
24. H. K. CHUANG and C. D. HAN, *Adv. Chem.* **206** (1984) 172.
25. K. MIN, J. L. WHITE and J. F. FELLERS, *Polym. Engng Sci.* **24** (1984) 1327.
26. W. J. MACKNIGHT, R. W. LENZ, P. V. MUSTO and R. J. SOMANI, *ibid.* **25** (1985) 1124.
27. C. D. HAN and H. K. CHUANG, *J. Appl. Polym. Sci.* **30** (1985) 2431, 2457.
28. L. A. UTRACKI, M. DUMOULIN and P. TOMA, *Polym. Engng Sci.* **26** (1986) 34.
29. L. D'ORAZIO, C. MANCARELLA, E. MARTUSCELLI, A. CASALE, A. FILIPI and F. SPERONI, *J. Mater. Sci.* **21** (1986) 989.
30. E. C. BERNHARDT, "Processing of Thermoplastic Materials" SPE Plastics Engineering Series (1974) p. 258.
31. H. J. YOO, *Polym. Engng Sci.* **27** (1987) 192.
32. H. BRODY, *J. Appl. Polym. Sci.* **31** (1986) 2753.
33. L. E. NIELSEN, "Mechanical Properties of Polymers and Composites", Vol. 2, Dekker, New York (1974) p. 285.
34. M. J. SHANKERNARAYANAN, D. C. SUN, M. KOJIMA and J. H. MAGILL, *Int. Pol. Processing* **1** (1987) 66.
35. B. BREW and I. M. WARD, *Polymer* **19** (1978) 1338.
36. M. A. HALLAM, D. L. M. CANSFIELD, I. M. WARD and G. POLLARD, *J. Mater. Sci.* **21** (1986) 4199.
37. P. G. ANDERSEN, S. H. CARR, *Polym. Engng Sci.* **16** (1976) 217.
38. J. W. LADBURY, *Plast. Instit., Trans.* **28** (1960) 184.
39. I. LEE, S. TURNER and R. T. WOODHAMS, *Pol. Compos.* **3** (1982) 212.
40. H. VOSS, J. H. MAGILL and K. FRIEDRICH, *J. Appl. Polym. Sci.* **33** (1987) 1745.
41. C. L. BEATTY and W. J. STAUFFER, *Adv. Chem.* **154** (1976) 112.
42. P. VAN GHELUWE, to be published.
43. A. RUDIN and H. P. SCHREIBER, *Polym. Engng Sci.* **23** (1983) 422.
44. D. CAMPBELL and M. M. QAYYUM, *J. Polym. Sci.* **18** (1980) 83.
45. L. BARTOSIEWICZ and C. J. KELLY, *Adv. Pol. Technol.* **7** (1987) 21.
46. S. L. SAKELLARIDES and A. J. McHUGH, *Rheol. Acta.* **26** (1987) 64.

Received 22 October 1988
and accepted 17 February 1988